**NASA Contractor Report** 178143

**ICASE REPORT NO.** 86-48



# ICASE

STABILITY AND CONTROL OF COMPRESSIBLE FLOWS
OVER A SURFACE WITH CONCAVE-CONVEX CURVATURE

Lucio Maestrello
Alvin Bayliss
Paresh Parikh
Eli Turkel

Contract Nos. NAS1-17070, NAS1-18107
July 1986



INSTITUTE FOR COMPUTER APPLICATIONS IN SCIENCE AND ENGINEERING
NASA Langley Research Center, Hampton, Virginia 23665

Operated by the Universities Space Research Association



National Aeronautics and
Space Administration
**Langley Research Center**
Hampton, Virginia 23665

# STABILITY AND CONTROL OF COMPRESSIBLE FLOWS OVER A SURFACE WITH CONCAVE-CONVEX CURVATURE

Lucio Maestrello
NASA Langley Research Center

Alvin Bayliss
Exxon Corporate Research Science Laboratories

Paresh Parikh
Vigyan Research Associates, Inc.

Eli Turkel
Tel-Aviv University, Tel-Aviv, Israel
and
Institute for Computer Applications in Science and Engineering

## ABSTRACT

The active control of spatially unstable disturbances in a laminar, two-dimensional, compressible boundary layer over a curved surface is numerically simulated. The control is effected by localized time-periodic surface heating. We consider two similar surfaces of different heights with concave-convex curvature. In one, the height is sufficiently large so that the favorable pressure gradient is sufficient to stabilize a particular disturbance. In the other case the pressure gradient induced by the curvature is destabilizing. It is shown that by using active control that the disturbance can be stabilized. The results demonstrate that the curvature induced mean pressure gradient significantly enhances the receptivity of the flow to localized time-periodic surface heating and that this is a potentially viable mechanism in air.

Research for the second and fourth authors was partially supported by the National Aeronautics and Space Administration under NASA Contract No. NAS1-17070 and NAS1-18107 while they were in residence at ICASE, NASA Langley Research Center, Hampton, VA 23665-5225.

Partial support was provided for the third author under NASA Contract No. NAS1-17919.

## 1. INTRODUCTION

In this paper, we simulate the development of spatially unstable disturbances in a compressible, two-dimensional laminar boundary layer over a curved surface. The curvature varies from concave to convex to flat over the length of the surface. The simulations are performed by numerically integrating the two-dimensional Navier-Stokes equations over the surface with a disturbance specified at the inflow. The objective is to investigate the stability and the active control of disturbances by localized, time-periodic surface heating in such a boundary layer. Our concern is with the nature of the instability of the time dependent disturbance interacting with the curvature induced mean pressure gradient, and with the ability to control the non-linear growth.

The concave part of the curvature is known to be potentially unstable to two- and three-dimensional disturbances while the convex part is stabilizing as a result of a favorable pressure gradient or acceleration (see Reynolds (1884); Liepmann (1943), and Schubauer and Skramstad (1947)). The overall effect of the surface curvature cannot be predicted a priori, as it will depend on the parameters of both the flow and of the disturbance. By geometrically shaping the surface, it is possible to achieve flow control, i.e., reduce the growth of disturbances. A reversion of a turbulent flow to a laminar flow is also possible (Narasimha and Sreenivasan, 1979). However, this technique has limited application in that it can be optimized only for a small range of flow parameters. A potentially less restricted method of control for a variety of flow conditions is by active means. Methods for the control of the flow are surveyed by Reshotko (1985).

The technique of actively controlling the growth of unstable waves by localized periodic surface heating was introduced by Liepmann, Brown, and Nosenchuck (1982) and by Liepmann and Nosenchuck (1982). The basic idea is to introduce a temperature disturbance out of phase from the propagating wave via a feedback mechanism and thereby induce a phase-amplitude cancellation. They demonstrated that the active control of instability waves using heating strips on the wall is an effective method for flow control in water. Maestrello and Ting (1985) analyzed this problem using the method of matched asymptotics as a "triple-deck" problem. The analysis confirmed that a small amount of localized active surface heating can excite local disturbances which increase the momentum near the wall and reduce the displacement thickness. This mechanism couples the surface heating to the flow. In other recent experiments in water, Lynch, Miller, Lewis, and Nosenchuck (1985) successfully controlled an artificially induced turbulent spot. In addition, Stuber, Dehpanah, and Gharib (1985) controlled the wake of an airfoil in a low Reynolds number flow.

In air, active control by surface heating is more difficult to achieve than in water. One reason is that the temperature-viscosity coupling is much weaker, thus requiring a higher temperature to impart an equivalent perturbation to the flow. It was shown by Maestrello (1986) that the disturbance required in air was 10-20 times larger than in water for an equivalent perturbation. This is consistent with experimental observations. In addition, only the unsteady portion of an imposed temperature disturbance contributes to control by proper phase adjustment, while the steady portion tends to destabilize (Schlichting (1968)). On the other hand, in water steady heating is stabilizing. As far as we are aware, active control in air by periodic surface heating has not been achieved experimentally.

In the above experiments, there was essentially no mean pressure gradient. The pressure gradient introduces a coupling of the mean flow with external disturbances (i.e., sound, vorticity or entropy disturbances) that is much stronger than in flows with no mean pressure gradient (e.g., Goldstein and Cowley (1986)). This coupling can induce large changes in the response of the mean flow to controlled disturbances, i.e., the receptivity of the flow is significantly enhanced. Maestrello (1986) found experimentally that a temperature disturbance placed near the leading edge of an airfoil can trigger instantaneous transition while a similar disturbance placed over the surface, where the pressure gradient is weaker, had a significantly reduced effect. Preliminary numerical results of the authors (Maestrello, Bayliss, Parikh, and Turkel (1985)) confirm the enhanced receptivity of flows with a non-zero mean pressure gradient to localized time-periodic surface heating.

Another means of active laminar flow control is the use of a vibrating ribbon. Milling (1981) and Thomas (1983), using a vibrating ribbon placed in the boundary layer, were able to delay transition by superimposing Tollmien-Schlichting waves of equal amplitude and opposite phase from the incoming growing disturbance.

In this paper, we study the effect of a curvature induced mean pressure gradient on the growth of laminar disturbances. In particular, we investigate the behavior of an imposed disturbance over two concave-convex surfaces with diferent heights. On one, the height is sufficiently large so that the favorable pressure gradient is sufficient to stabilize a particular disturbance. Hence, we have passive control by geometrical shaping. For the other surface, the favorable pressure gradient is not sufficient to overcome the effect of the unfavorable pressure gradient, thus the net effect is

destabilizing. We show that control of this instability can be successfully achieved using active surface heating.

In section 2, the numerical method is described. In section 3, we present the numerical results and discussion. Finally, in section 4, the conclusions are presented.

## 2. NUMERICAL METHOD AND COMPUTATIONAL MODEL

In this section we present the numerical method and other aspects of the computational model. We consider the compressible, two-dimensional Navier-Stokes equations. In Cartesian coordinates, x and y, these equations can be written in the conservation form

$$W_t = \tilde{F}_x + \tilde{G}_y \tag{2.1}$$

where $W$ is the vector $(\rho, \rho u, \rho v, E)^T$, $\rho$ is the density, $u$ and $v$ are the $x$ and $y$ components of the velocity respectively, and $E$ is the total energy. The functional forms of the flux functions $\tilde{F}$ and $\tilde{G}$ are standard and will not be given here for brevity. The system (2.1) is supplemented by the equation of state for an ideal gas

$$p = \rho RT,$$

where $p$ is the pressure, $T$ the temperature, and $R$ is the gas constant. Sutherland's law is used for the variation of viscosity with temperature $\mu(T)$.

In order to deal with surface curvature we introduce a general, non-orthogonal coordinate transformation

$$\begin{aligned} \xi &= \xi(x,y) \\ \eta &= \eta(x,y) \end{aligned} . \tag{2.2}$$

The wall is the curve $\eta = 0$. Applying the transformation (2.2), the system (2.1) is transformed to the new system

$$(JW)_t = F_\xi + G_\eta \tag{2.3}$$

where $J$ is the Jacobian

$$J = x_\xi \, y_\eta - x_\eta \, y_\xi$$

and the new flux functions $F$ and $G$ are given by

$$F = \tilde{F}y_\eta - \tilde{G}x_\eta \quad \text{and} \quad G = \tilde{G}x_\xi - \tilde{F}y_\xi .$$

The transformed system (2.3) is solved by an explicit finite difference scheme using a rectangular $(\xi,\eta)$ grid in the computational plane. The viscous stresses must be transformed to the new coordinate system. The precise form of the transformed system of equations is omitted for brevity. Assuming that the wall is a single-valued function of $x$, described by the equation,

$$y = f(x),$$

the coordinate transformation used is

$$\xi = x \tag{2.4a}$$

$$\eta = \frac{(y - f(x))}{(y_T - f(x))} y_T \tag{2.4b}$$

where $y_T$ is the top of the computational domain. An additional exponential stretching is applied to (2.4b) to increase the grid resolution near $\eta = 0$ where large variations in the solution have to be resolved. The transformation (2.4) is not orthogonal near the wall; however, the types of curvature considered in this paper are not particularly severe and the transformation (2.4) is believed to be adequate.

The finite difference scheme is a modification of the MacCormack scheme making it fourth-order accurate on the convective terms. The scheme is second-order accurate in time and is second-order on the viscous terms for non-constant viscosity. The fourth-order accuracy is essential in order to:

a) prevent viscous-like truncation errors on the convective terms from artificially decreasing the effective Reynolds number of the computation, and

b) prevent numerical dispersion and dissipation from altering the character of the waves which are computed in the mean flow.

The numerical scheme is described in detail in Bayliss, Parikh, Maestrello, and Turkel (1985a). The discussion below will therefore be short. The numerical scheme applied to the one-dimensional equation

$$u_t = F_x$$

consists of a predictor of the form

$$\bar{u}_i = u_i^N + \frac{\Delta t}{6\Delta x}\left(-7F_i + 8F_{i+1} - F_{i+2}\right) \tag{2.5a}$$

together with a corrector of the form

$$u_i^{N+1} = \frac{1}{2}\left(\bar{u}_i + u_i^N + \frac{\Delta t}{6\Delta x}\left(7\bar{F}_i - 8\bar{F}_{i-1} + \bar{F}_{i-2}\right)\right). \tag{2.5b}$$

In (2.5) the subscript $i$ denotes the spatial grid point and the superscript $N$ denotes the time level. The scheme (2.5) is alternated with the symmetric variant.

Two-dimensional problems are treated by operator splitting. For example, if $L_x$ denotes the solution operator symbolized by (2.5) for the equation

$$W_t = F_x,$$

and $L_y$ denotes the similar operator for the equation

$$W_t = G_y,$$

then the solution to the equation

$$W_t = F_x + G_y$$

is obtained by

$$W^{N+2} = L_x L_y L_y L_x W^N. \tag{2.6}$$

The split scheme (2.6) preserves the second-order accuracy in time and the fourth-order accuracy in space. In the applications the scheme described above is applied to the transformed system (2.3).

A typical computational domain is shown in Figure 1. We first solve the Navier-Stokes equations on a coarse grid using constant inflow data. This grid is sufficient to resolve the mean flow but not the unstable Tollmein-Schliting waves associated with the mean flow. The equations are marched in time until a steady-state solution is obtained. This solution is then interpolated to a finer grid which is sufficiently fine to resolve the unstable Tollmein-Schlichting waves. It is possible that a steady state would not be numerically achieved by time marching techniques if the mesh were fine enough to resolve the unstable waves. The numerical code is then run with a time dependent disturbance specified at the inflow and with the interpolated steady state used as the initial condition. The specified inflow boundary data is of the form

$$W_{inflow} = W_0 + \varepsilon \, \mathrm{real}\left(e^{i\omega t} H(y)\right) \tag{2.7}$$

where $W_0$ is the interpolated steady state, $\omega$ is the frequency, $H(y)$ is a complex solution of the Orr-Sommerfeld equation for a given boundary layer profile at the specified inflow Reynolds number, and $\varepsilon$ is used to adjust the amplitude of the fluctuating disturbance. The profiles $H(y)$ used here were obtained from a program developed at NASA Langley Research Center by J. R. Dagenhart.

The numerical treatment of the boundaries involves extrapolating the outgoing characteristics from the interior, in addition to imposing

appropriate data. The reader is referred to Bayliss et al. (1985a) for further details. In order to complete the specification of the model we discuss the boundary conditions that are imposed.

At the inflow (see Figure 1) an unsteady disturbance based on an incompressible Orr-Sommerfeld profile is imposed as described above. At the wall the velocities are set to zero and the temperature is specified to be the free-stream stagnation value. Active surface heating is modelled by locally modifying the temperature boundary condition. The functional form that we use to model the heating and cooling strips will be described later.

Both the outflow and upper boundaries are subsonic and if we neglect viscosity, one boundary condition must be imposed because there is one incoming characteristic entering the computational domain. The boundary condition is chosen so that the time derivative of the incoming one-dimensional normal characteristic variable is zero. For example, at the upper boundary we impose

$$p_t - \tilde{\rho}\tilde{c}v_t = 0 \tag{2.8}$$

where $\tilde{c}$ is the sound speed and $\tilde{\rho}$ and $\tilde{c}$ are taken from the previous time step. At the outflow boundary we impose

$$p_t - \tilde{\rho}\tilde{c}u_t = 0 \tag{2.9}$$

corresponding to the characteristic entering the domain from $x = +\infty$.

The use of the one-dimensional characteristic absorbing boundary condition, such as (2.9), is a common practice in wave propagation problems

(see Cohen, Hughes, and Jennings (1981)). This condition does not account for waves with a variable dispersion relation generated by the viscous boundary conditions. In practice we do not use data from a small region around the outflow boundary. We have verified that (2.8) and (2.9) do not affect the solution for the position of the artificial boundaries and the time intervals used in the computation. This is based on:

(a) The ability of the code to reproduce growth rates and phase velocities predicted by linear theory (for sufficiently small inflow disturbances);

(b) No visible reflections in specific profiles examined as a function of time;

(c) Moving the position of the artificial boundaries and verifying that the solution is insensitive to the position of these boundaries.

## 3. RESULTS

In this section we present numerical results for two curved surfaces. The configurations are shown in Figure 2. They differ primarily in the height of the surface at the outflow boundary and also in the degree of curvature. In both cases the computational domain extends for a distance of 2.4 ft. in the stream-wise direction. The curved part of the surface extends for a distance of 1.2 ft. from the inflow and then becomes flat. The shape of the surface is defined by a fourth-degree polynomial which is designed to become flat smoothly at the inflow ($x = 0$) and at the position of the maximum height ($x = 1.2$ ft.) (see Maestrello et al. (1985)).

Unless otherwise stated, all of the present results are for an inflow Mach number, $M_\infty$ of 0.7, unit Reynolds number based on the free stream values (Re/Ft), of $3.0 \times 10^5$ (corresponding to an inflow Reynolds number based on the displacement thickness, $Re_\delta^*$, of 896) and stagnation temperature of $520^oR$. The final heights for the two configurations are 0.02 ft. and 0.04 ft. respectively. The boundary layer thickness at inflow $(\delta_i)$ is .0095 ft. The free stream velocity accelerates to $M_\infty = 0.725$ (configuration 1) and 0.76 (configuration 2) respectively. The final heights represent a significant perturbation compared to the boundary layer thickness and therefore the curvature affects the viscous stability of the flow even though the far field acceleration is not large. The Reynolds numbers based on the final heights $\left(Re = U_\infty h/\nu_\infty\right)$ are 6170 and 12,850 respectively.

The configurations were selected to illustrate the effect of the curvature induced mean pressure gradient on the stability of the boundary layer. In both configurations the curvature is initially concave causing a compression and a resulting destabilization. Further downstream the curvature becomes convex leading to an expansion with a resulting stabilization. Configuration 2 is twice as high as configuration 1, and the average slope of configuration 2 is twice that of configuration 1. As a result, the favorable pressure gradient is much larger for configuration 2 than configuration 1.

In the first part of this section we study the behavior of uncontrolled disturbances around both configurations. With configuration 2, the favorable pressure gradient is sufficient to stabilize the flow over the flat portion of the surface. With configuration 1, the favorable pressure gradient is weaker, and the disturbance amplitude is sufficiently large ($\varepsilon = 0.02$) so that the disturbance exhibits strong nonlinear growth over the flat portion of the

surface. Thus, the net effect of the curvature is destabilizing. In the second part of this section, we demonstrate that with active control by periodic surface heating, the flow over configuration 1 can be stabilized.

In the remainder of this section we will present results obtained from numerically computing both the mean flows associated with these configurations and the unsteady flow obtained from forcing the mean flow with an unsteady perturbation at the inflow and from imposing unsteady temperature disturbances on the surface as an active control mechanism. The code has been validated in two ways. In Bayliss, Maestrello, Parikh, and Turkel (1985b) it was shown that the growth (and decay) rates predicted from linear theory could be reproduced for sufficiently small inflow disturbances. (This was for a freestream Mach number of 0.4.) In addition, the results described below were verified by mesh refinements.

We first discuss the mean flow solution and the uncontrolled, unsteady results.

## Mean and Uncontrolled Results

The mean free stream Mach number $M_e$ and the pressure coefficient $C_p = (p - p_{\infty i})/(\frac{1}{2}\rho_{\infty i}U^2_{\infty i})$ are shown in Figure 2 for both configurations. Here and below the subscripts e, $\infty$, and i refer to the edge of the boundary layer, free stream and inflow conditions respectively. It is apparent that configuration 1 has a significant adverse pressure gradient while configuration 2 allows a large acceleration and favorable pressure gradient due to the increased height of the surface.

We next consider the unsteady flow obtained by introducing time-periodic disturbances at the inflow in the manner discussed above. The non-dimensional frequency $F\ (= 2\pi f\ \nu/U_{\infty i}^2)$ is $0.8 \times 10^{-4}$. Based on the incompressible, linear stability theory for a flat-plate, this frequency is unstable. Here, $f$ is the frequency and $\nu$ the kinematic viscosity. The maximum perturbation at the inflow is 2% of the freestream velocity.

In Figure 3a we plot the growth of the unsteady disturbance as a function of $x$ for both configurations and compare with the growth obtained over a flat plate of the same length. The growth of the disturbance is obtained by computing the RMS of the fluctuating momentum, integrating the result across the boundary layer and normalizing by the value at the inflow $\left(\sqrt{\overline{(\rho u)^2}}^{\,*}\right)$. The results in Figure 3a were obtained using an identical inflow in all three cases.

As can be seen, the behavior of the unsteady disturbance is very different for the two configurations. In both cases the disturbance is initially amplified due to the unfavorable pressure gradient. For configuration 2, it appears that the favorable pressure gradient is sufficient to significantly reduce the level of the fluctuation so that over the flat portion there is no growth. In contrast, for configuration 1, the favorable pressure gradient is weaker and there is a much smaller reduction in amplitude up to the flat portion of the surface ($x$ = 1.2 ft.), with a strong exponential-like growth over the flat portion. In summary, the pressure gradient induced by configuration 1 is destabilizing while the pressure gradient induced by configuration 2 is stabilizing.

A very similar stability phenomenon has been observed for flows over a flat surface at two different Mach numbers. Computations were performed for flows at $M = 0.7$ and $M = 0.4$ (Bayliss et al. 1985b). The inflow Reynolds number ($Re_w^*$) and the amplitude of the perturbation at the inflow were the 1000 and 2% respectively. Note that this inflow $Re_w^*$ is different from that of Figure 3a which accounts for the difference in the growth rates for $M_B = 0.7$ in two figures. In the case of $M = 0.7$ the disturbance first grew and then decayed while for $M = 0.4$ the disturbance exhibited strong exponential growth over the entire length of the surface. This is illustrated in Figure 3b taken from Bayliss et al. (1985b). These results demonstrate, for two different geometries, the stabilizing effect of increasing the Mach number.

The growth observed in Figure 3b for $M = 0.4$ is a nonlinear effect. Reducing the amplitude of the inflow disturbance eliminated it. This behavior was explained by an analysis of Goldstein and Durbin (1986). They showed that nonlinear effects eliminated the upper branch of the stability curve. We have not investigated the effect of reducing the disturbance amplitude for configuration 1, but it is reasonable to assume that the growth exhibited in Figure 3a is a nonlinear effect of the type analyzed by Goldstein and Durbin (1986).

The destabilizing effects of the surface curvature are also illustrated in Figures 4 and 5 where we plot the vorticity contours at a fixed instant of time for configurations 1 and 2 respectively. In both cases the figures indicate significant velocity gradients over the initial portion of the curved surface where there is an unfavorable mean pressure gradient. However, further downstream, Figure 5 shows a dramatic reduction in the size of the

perturbation, as compared to Figure 4. This is clearly a consequence of the stabilization caused by the large favorable mean pressure gradient of configuration 2.

## Control Results

We model surface heating and cooling by modifying the temperature boundary condition over a small portion of the surface. In this paper we consider the control strip located in the region of unfavorable pressure gradient centered around x = 0.3 ft. Some preliminary results for the effects of surface heating and cooling in flows with both favorable and unfavorable pressure gradients were presented by Maestrello et al. (1985).

The length of the control strip is roughly 10% of the wavelength of the disturbance at the inflow. For control, the temperature is modified according to the formula

$$\frac{T}{T_{ref}} = \frac{T_w}{T_{ref}} \pm \left(\alpha + \beta^2 \sin^2\left(\frac{Ft}{2} + \phi\right)\right) \qquad (3.1)$$

where the plus sign is for heating and the minus sign is for cooling, $T_w$ is the temperature at the wall ($520^oR$), $T_{ref}$ is the reference temperature, and F is the non-dimensional frequency ($0.8 \times 10^{-4}$). The functional form of (3.1) models resistive heating with a DC current ($\alpha$) and an AC current ($\beta$). The phase $\phi$ is varied to investigate the effectiveness of active control.

The parameters for the heating case are $\alpha = 1.0$, $\beta = 2.76$ corresponding to a peak temperature of $1650^oR$. For the cooling case, the parameters are

$\alpha = 0.77$, $\beta = 1.7$ corresponding to a minimum temperature of $190^{\circ}R$. In the heated case, the maximum temperature is roughly three times the unheated wall temperature which is close to the temperature used in the experiment of Maestrello (1985) using a tungsten wire. There were no numerical instabilities due to the large temperature perturbations but the heating forced a reduction in the allowable time step. In the cooled case, the parameters are chosen so that the temperature will stay within a range where Sutherland's law is valid for the viscosity as a function of temperature. We note that such a periodic cooling is not attainable by experimental techniques available at the present time except for extremely low frequencies.

In Figures 6 and 7 we plot the RMS momentum flux $\sqrt{\overline{\rho u^2}}^{*}$ for heating and cooling respectively. In each case we consider two extreme phases, corresponding to a controlling disturbance being in and out of phase with the unstable wave, and compare with the uncontrolled results. We did not make a systematic study of other phases for optimization.

The results in Figure 6 demonstrate that depending upon the phase, active heating can either enhance or reduce the amplitude of the disturbance. In particular, the phase of the heating can be chosen to reduce the disturbance level to the point that there is no growth over the flat portion. In this case, the phase is $\phi = 0^{0}$, corresponding to an out of phase signal. It is remarkable that a single heating strip can induce such a dramatic change in the behavior of the unsteady disturbance. This is to be contrasted with the relatively modest control the authors were able to obtain over a flat geometry with zero mean pressure gradient (see Bayliss et al. (1986)). The results illustrate the enhanced receptivity due to the mean pressure gradient. Even

though the present control relates to a single frequency disturbance, it is not unreasonable to assume that a more complex flow can be controlled using multiple strips. In fact, Lynch et al. (1985) were able to control a turbulent spot in a water tunnel using multiple elements. As would be expected the opposite phase, $\phi = 90^0$, amplifies the unsteady disturbance. This suggests that localized, periodic surface heating can be used to trip the boundary layer. Maestrello (1985) used this technique to effect instantaneous transition by using a heating element on the leading edge of an airfoil.

The results for active cooling, Figure 7, are less dramatic but still indicate the effect of phase. In this case, the magnitude of the control temperature was roughly 1/3 that for the heating case.

The instantaneous total vorticity for the controlled case, with out of phase heating, is shown in Figure 8. Large reduction in the level of the vorticity is evident as compared to the uncontrolled case, Figure 4. In particular, this reduction is significant over the curvature and extending on to the flat portion. In Figure 9, time traces of $\rho u(t)$ as a function of non-dimensional time $t\, u_\infty/L$ are shown at four different positions across the boundary layer, where $L$ is the reference length. The effectiveness of control is further illustrated where the RMS of the mass fluctuation $\sqrt{\overline{(\rho u)^2}}$ is plotted as a function of $y/\delta_i$ for both the controlled and the uncontrolled cases. The results (see especially $\frac{y}{\delta} = 0.806$) not only show the reduction in amplitude due to the active control, but that nonlinear distortion present in the uncontrolled solution is almost completely eliminated by the active control. This shows that the flow has been brought back into the linear regime.

## 4. CONCLUSIONS

The growth and decay of spatially unstable disturbances in a compressible boundary layer over a concave-convex surface is dependent upon the overall mean pressure gradient induced by the curvature and by the parameters of the disturbance. In both the configurations studied, the disturbance initially amplifies due to the concave curvature and then decays in the region of the favorable mean pressure gradient induced by the convex curvature. It is observed that for the configuration with a larger favorable mean pressure gradient, the stabilizing effect is large enough to reduce the growth significantly. This is a form of passive control by geometrical shaping. It has limited application and may have adverse effect on the total drag.

For the configuration with smaller favorable mean pressure gradient, the flow is not stabilized. For this case it is shown that active control using localized periodic surface heating is a viable technique to achieve flow control. In contrast with our earlier study with zero mean pressure gradient (Bayliss et al. (1985a)), it is demonstrated that the receptivity of the flow is enhanced. Active control is a more flexible control mechanism than passive methods, because the phase and amplitude, over a range of frequencies can be controlled by matching to the unstable wave to cancel existing disturbances.

In practice, active surface heating would be applied with multiple heating strips and with temperature signals that are synthesized by a feedback control mechanism. In addition, the unstable disturbances may not be periodic and may have significant three-dimensionalities. In such a case, distributed control may have to be used with non-periodic signals and phase variation in the spanwise direction.

**ACKNOWLEDGEMENT**

The authors wish to thank Professor E. Reshotko for critically reviewing the manuscript.

## REFERENCES

BAYLISS, A., MAESTRELLO, L., PARIKH, P. and TURKEL, E. (1986), Numerical simulation of boundary layer excitation by surface heating/cooling. AIAA-85-0565, to appear in AIAA J.

BAYLISS, A., PARIKH, P., MAESTRELLO, L., and TURKEL, E. (1985a), A fourth order scheme for the unsteady compressible Navier-Stokes equations. AIAA-85-1694.

BAYLISS, A., MAESTRELLO, L., PARIKH, P., and TURKEL, E. (1985b), Wave phenomena in a high Reynolds number compressible boundary layer. Proc. of Workshop on Stability of Time-Dependent Flows, Springer-Verlag.

COHEN, M. F., HUGHES, T. J. R., and JENNINGS, P. C. (1981), A comparison of paraxial and viscous silent boundary methods in finite element analysis. Proceedings of the joint ASME-ASCE Conference, University of Colorado, 67-80.

GOLDSTEIN, M. E. and COWLEY, S. J. (1986), The generation of Tollmien-Schlichting waves in noninteractive marginally separated flows, Manuscript for Physics of Fluids.

GOLDSTEIN, M. E. and DURBIN, P. A. (1986), Nonlinear critical layers eliminate the upper branch of spatially growing Tollmein-Schliting waves. Manuscript for Physics of Fluids.

LIEPMANN, H. W. (1943), Investigations on laminar boundary layer stability and transition on curved boundaries. NACA, Wartime Rep. W107 (ACR 3M 30).

LIEPMANN, H. W., BROWN, G. L. and NOSENCHUCK, D. M. (1982), Control of laminar-instability waves using a new technique. J. Fluid Mech., **118**, 187-200.

LIEPMANN, H. W. and NOSENCHUCK, D. M. (1982), Active control of laminar turbulent transition. J. Fluid Mech., **118**, 201-204.

LYNCH, M. K., MILLER, P., LEWIS, C. and NOSENCHUCK, D. M. (1985), Visualization of active turbulent boundary layer control using a scanning laser sheet. Bull. Amer. Phys. Soc., **30**, 10, 1751.

MAESTRELLO, L. (1986), Active transition fixing and control of boundary layer in air. AIAA-85-0564, to appear in AIAA J.

MAESTRELLO, L. and TING, L. (1985), Analysis of active control by surface heating. AIAA J., **23**, 7, 1038-1045.

MAESTRELLO, L., BAYLISS, A., PARIKH, P., and TURKEL, E. (1985), Active control of compressible flows on a curved surface. SAE Technical Paper 851856.

MILLING, R. W. (1981), Tollmien-Schlichting wave cancellation. Phys. Fluids, **24**, 979-981.

NARASIMHA, R. & SREENIVASAN, K. R. (1979), Relaminarization of Fluid Flows. Adv. in Appl. Mech., **19**, 221-308.

RESHOTKO, E. (1985), Control of Boundary Layer Transition. AIAA Shear Flow Control Conf., AIAA-85-0562.

REYNOLDS, O. (1884), The two manners of motion of water. Proc. Royal Inst. Great Britain, 11.

SCHLICHTING, H. (1968), Boundary Layer Theory, McGraw-Hill Company.

SCHUBAUER, G. B. and SKRAMSTAD, M. K. (1947), Laminar boundary layer oscillations and stability of laminar flow. J. Aeron. Sci., **14**, 69.

STUBER, K., DEHPANAH, K., and GHARIB, M. (1985), Modification of vortex patterns in low Reynolds number wakes. Bull. Amer. Phys. Soc., **30**, 10, 1727.

THOMAS, A. S. W. (1983), The control of boundary layer transition using a wave-superposition principle. J. Fluid Mech., **137**, 233-250.

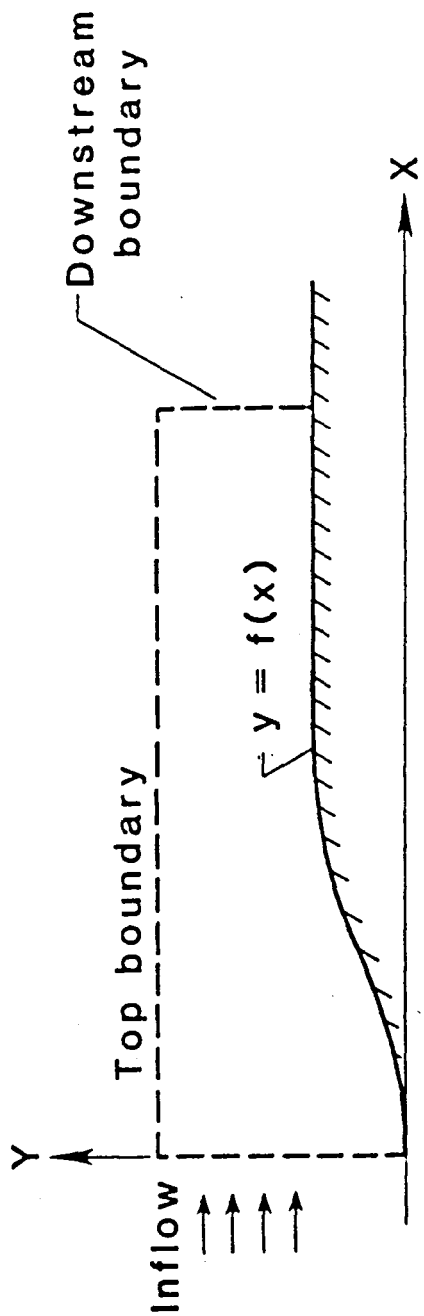


Figure 1. Computational Domain.

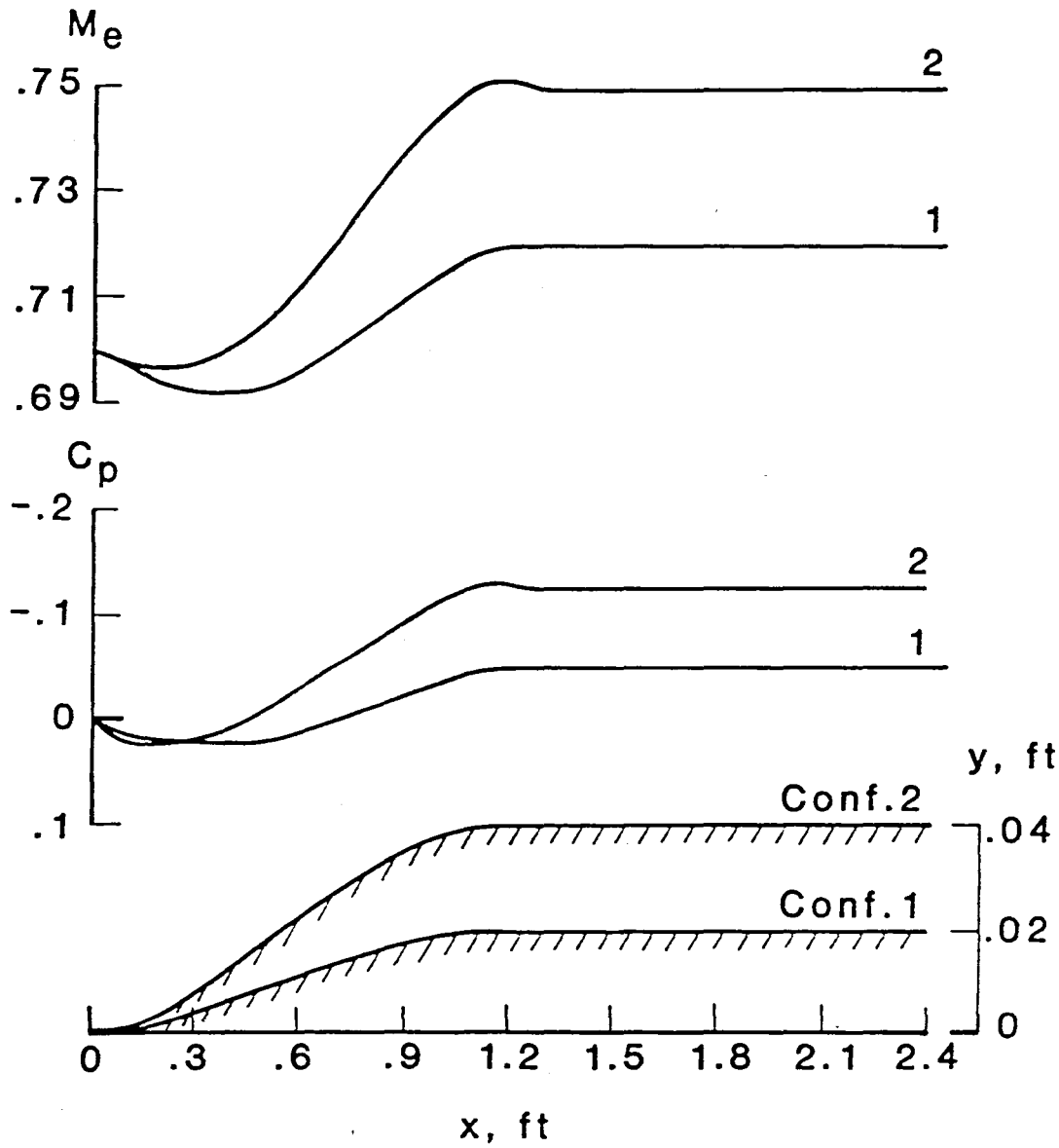


Figure 2. Mach Number and Pressure Distribution.

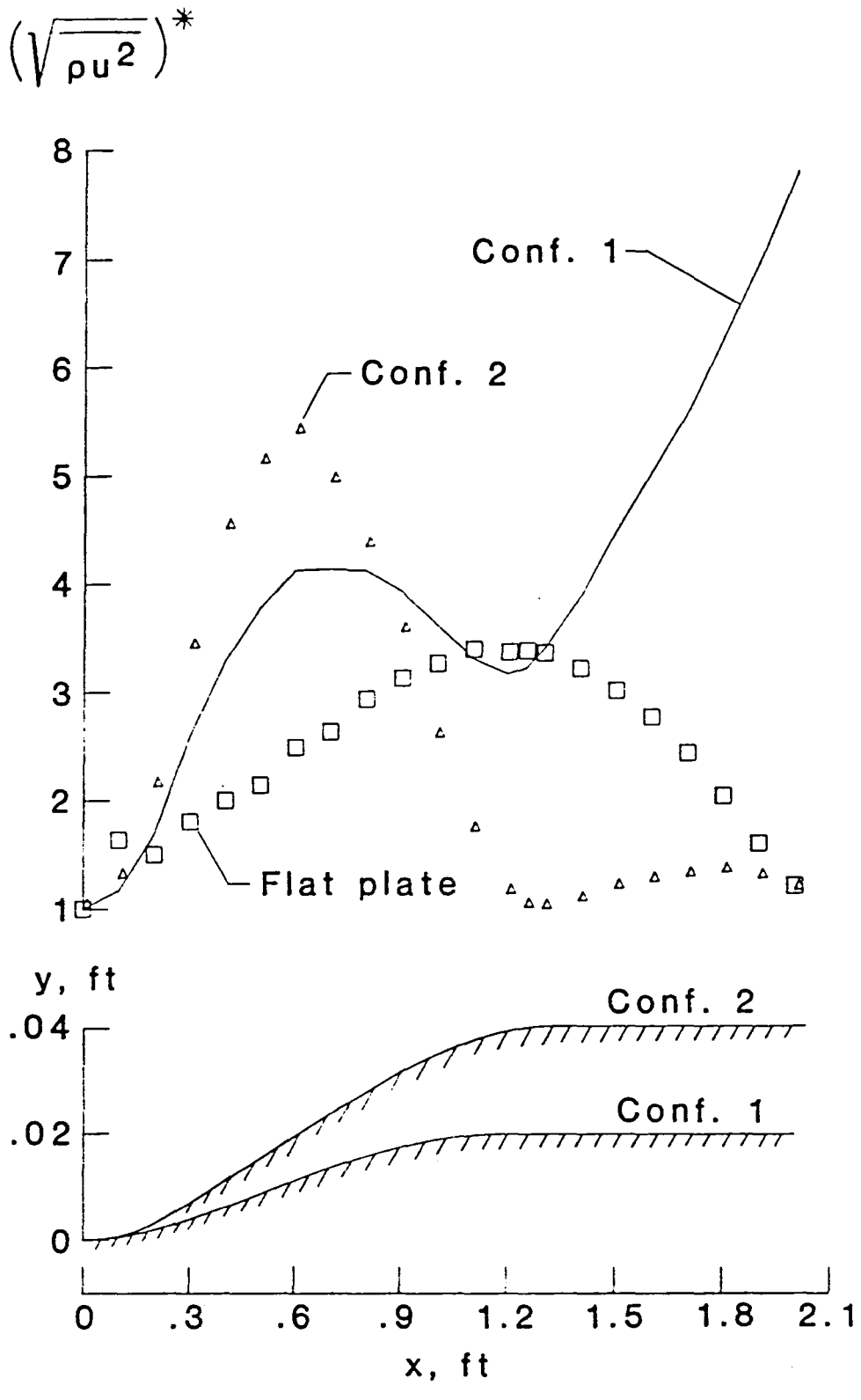


Figure 3a. Comparison of Amplitude Growth Between Curved Surfaces and a Flat Plate. Inflow $R_{e_\delta}{}^*$ = 896.

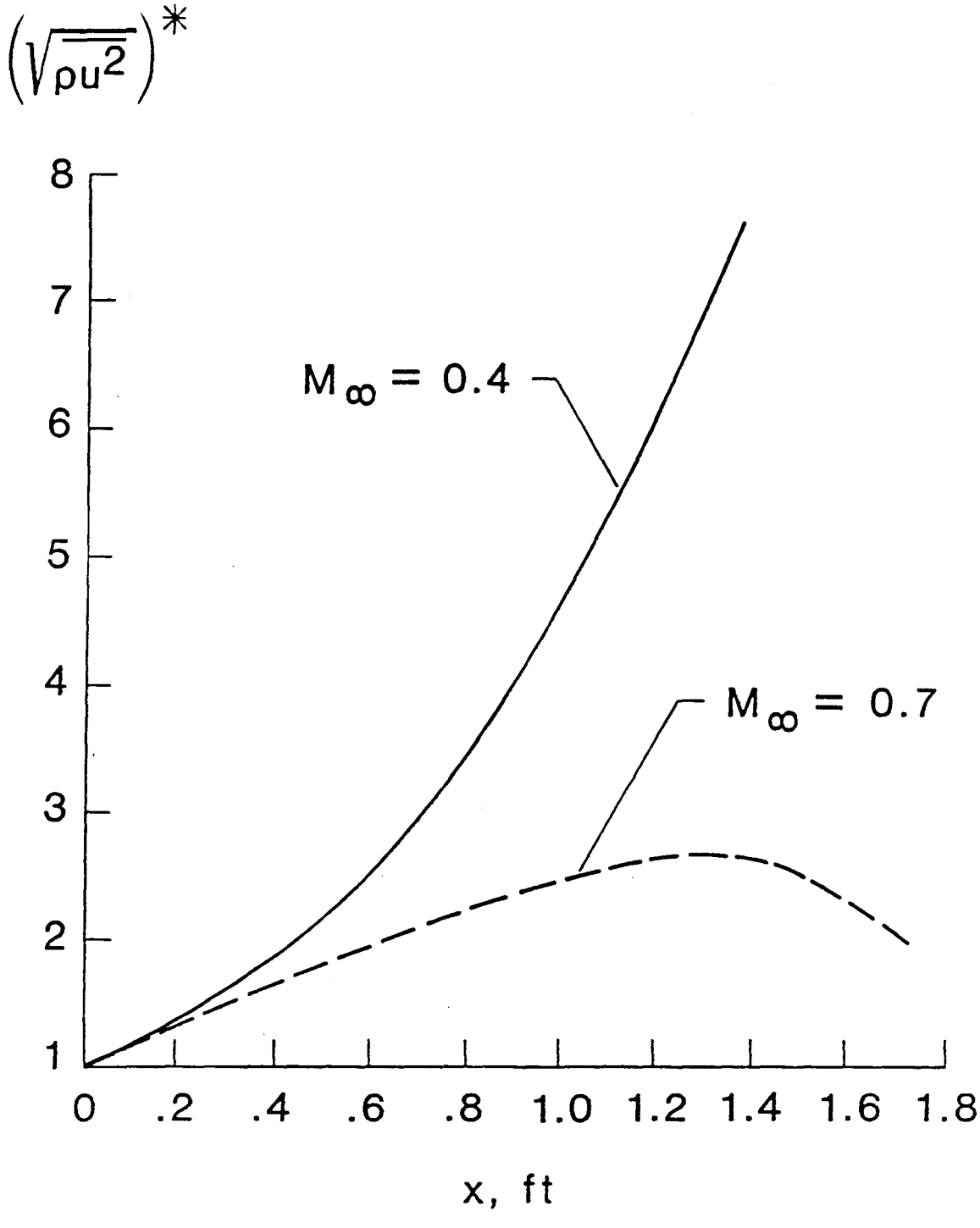


Figure 3b. Effect of Mach Number on Amplitude Growth. Inflow $R_{e_\delta}{}^* = 1000$.

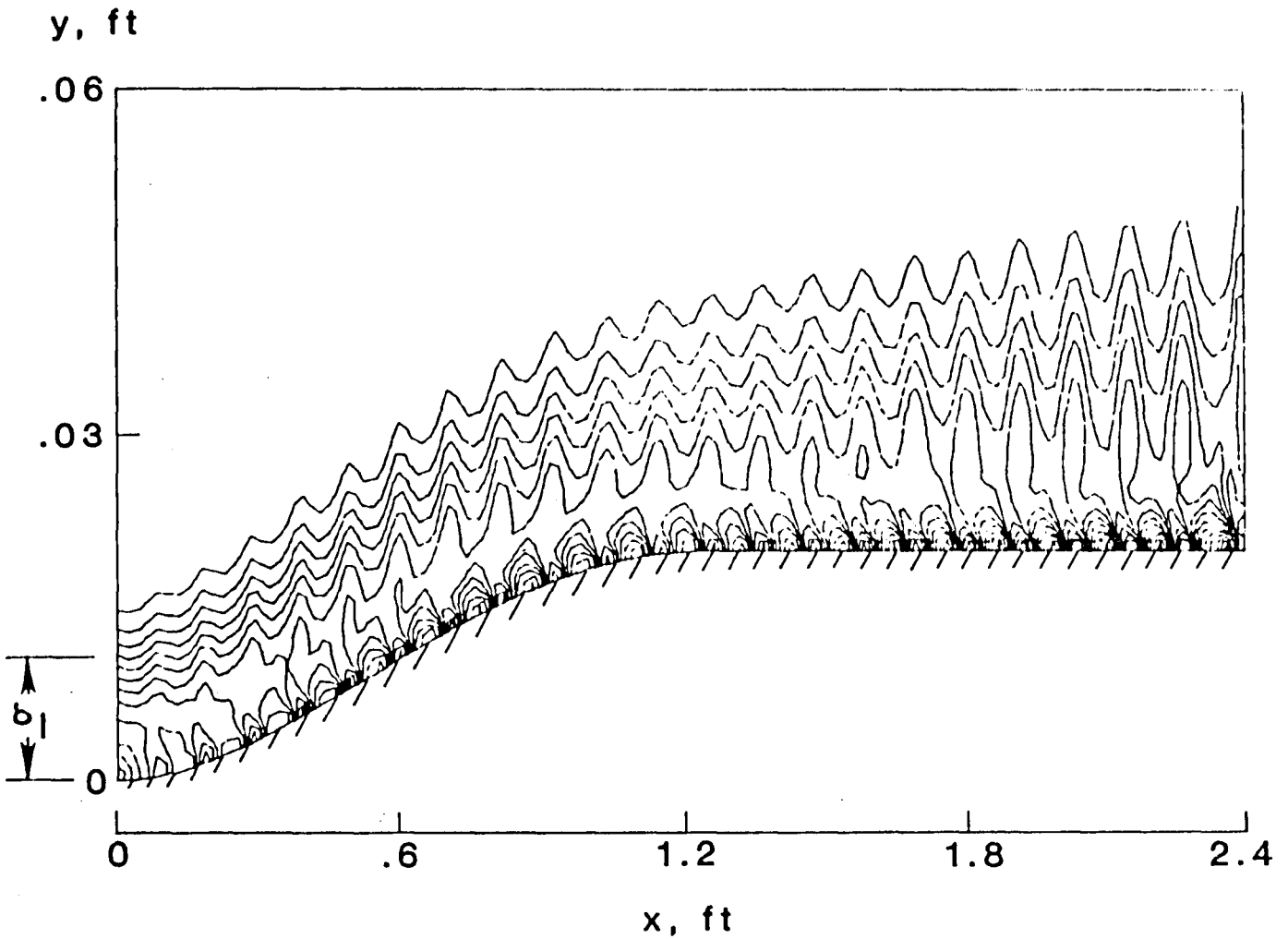


Figure 4. Instantaneous Total Vorticity Contours, Configuration 1.

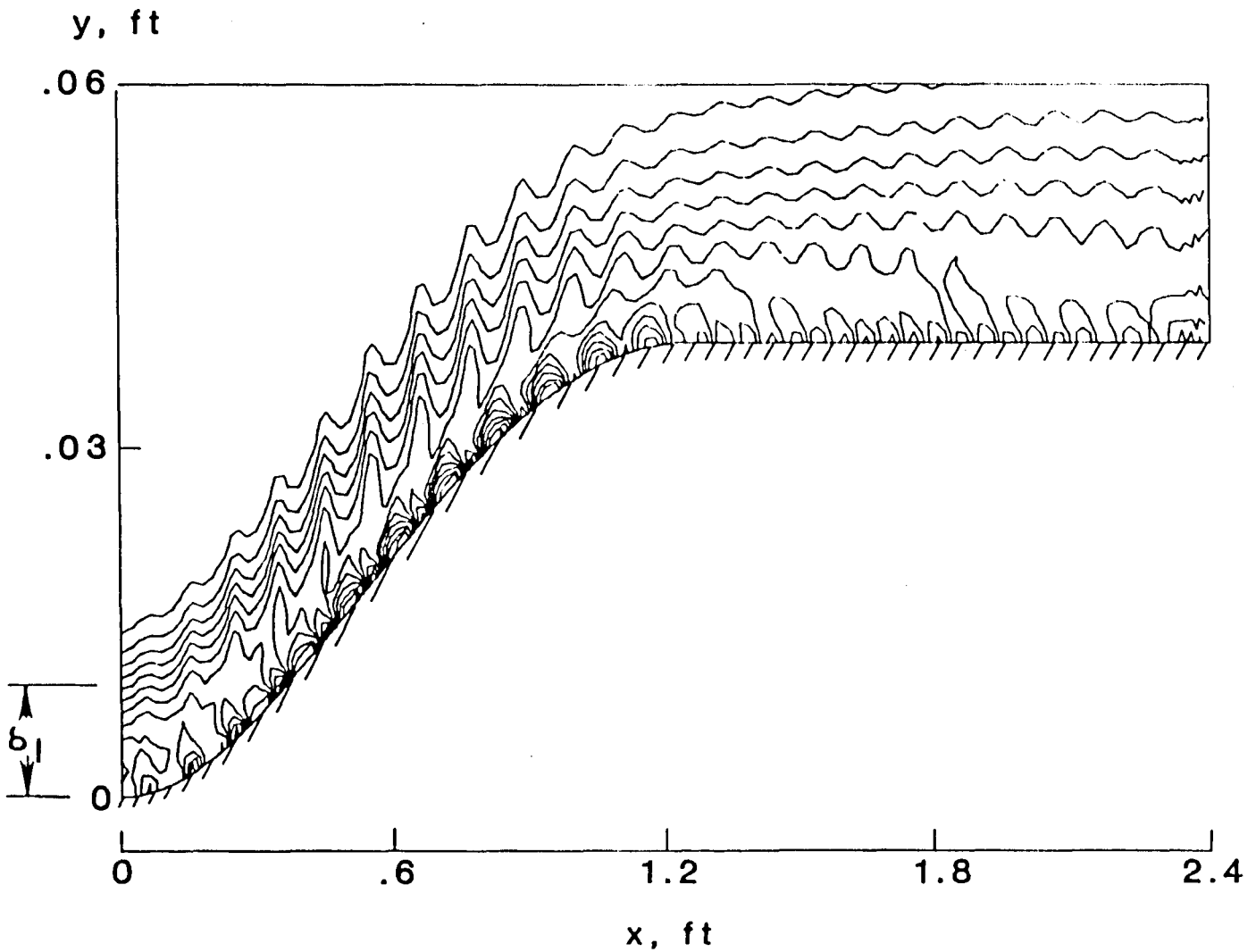


Figure 5. Instantaneous Total Vorticity Contours, Configuration 2.

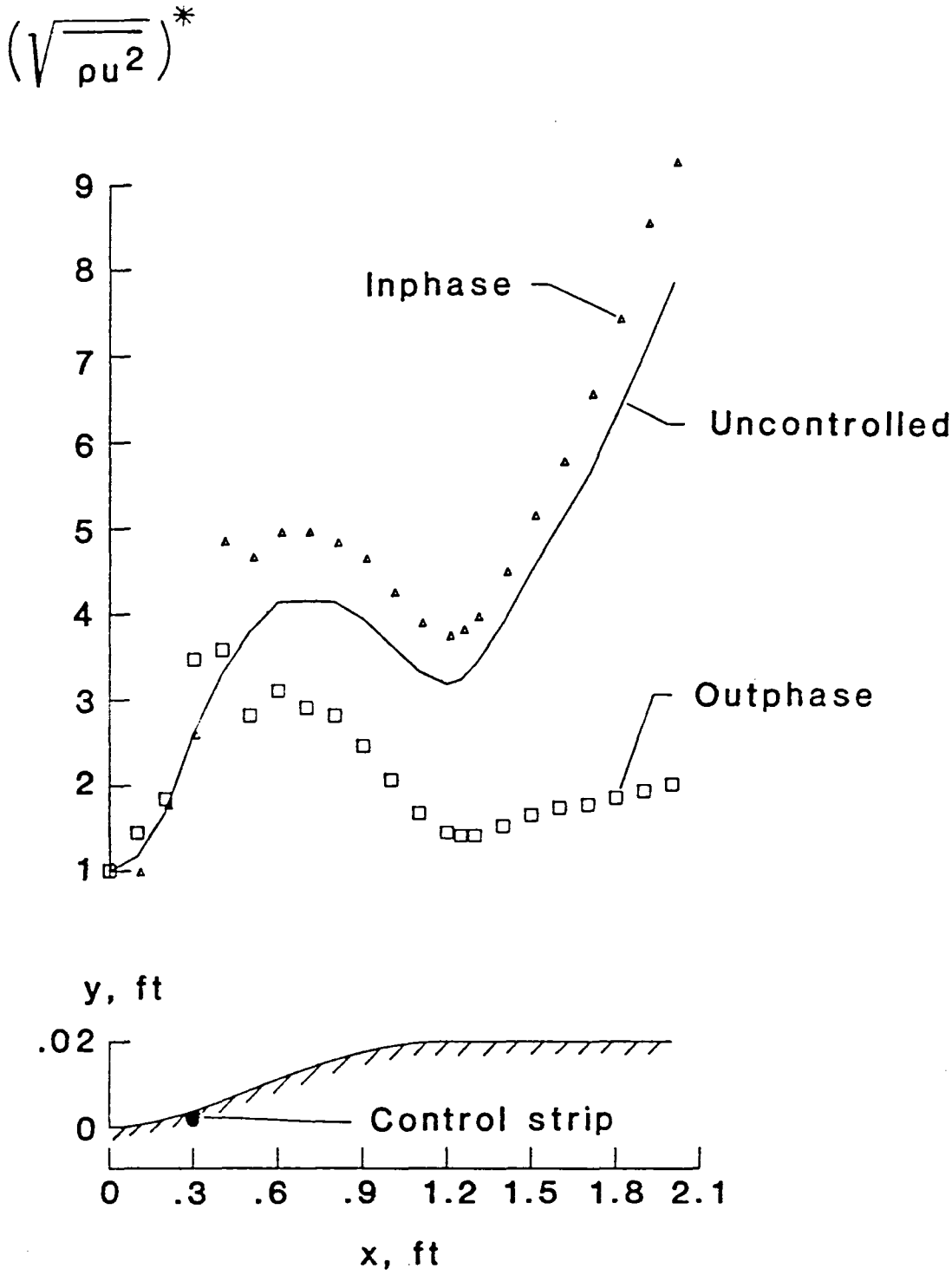


Figure 6. Amplitude Growth With and Without Control by Heating, Configuration 1.

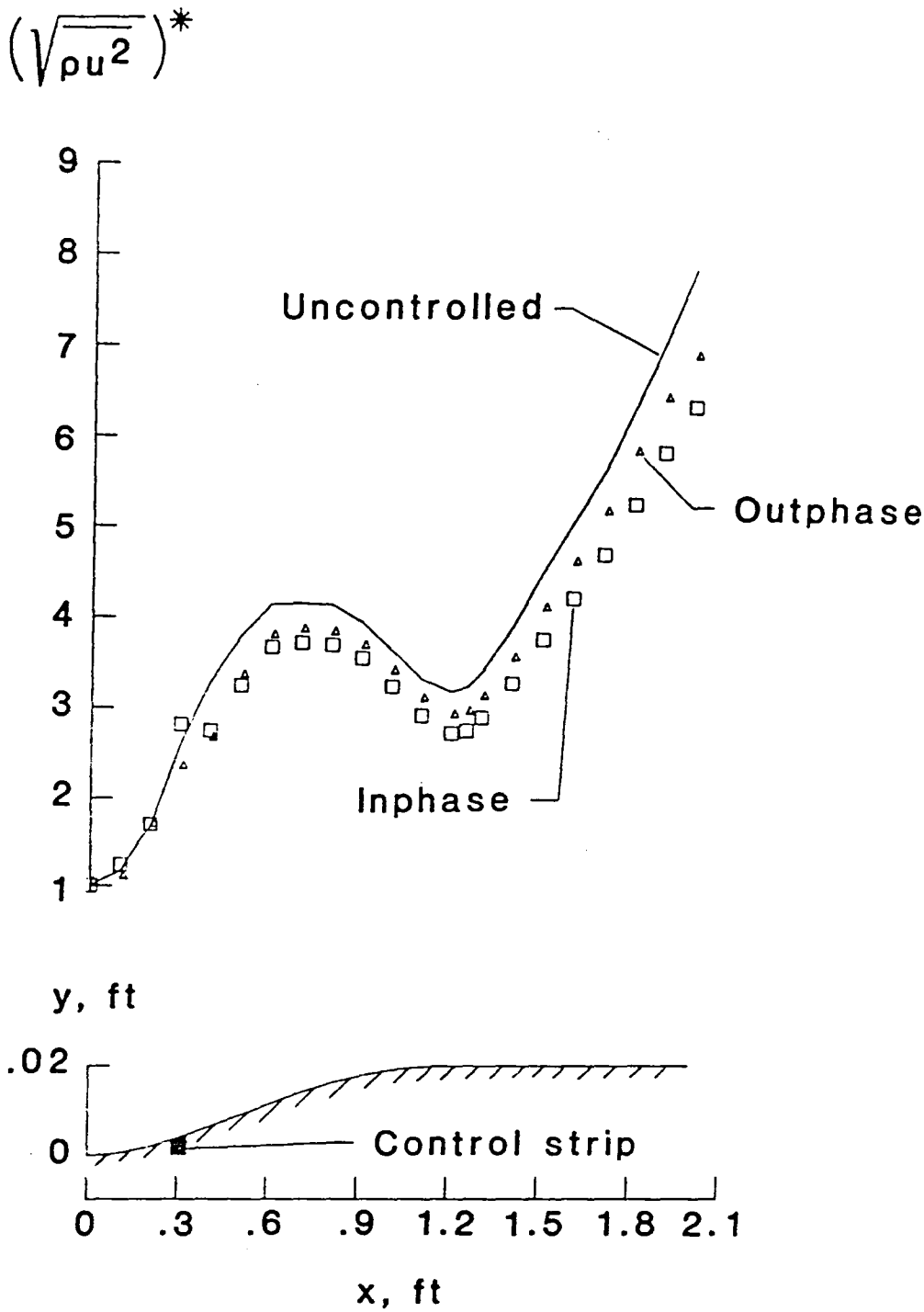


Figure 7. Amplitude Growth With and Without Control by Cooling, Configuration 1.

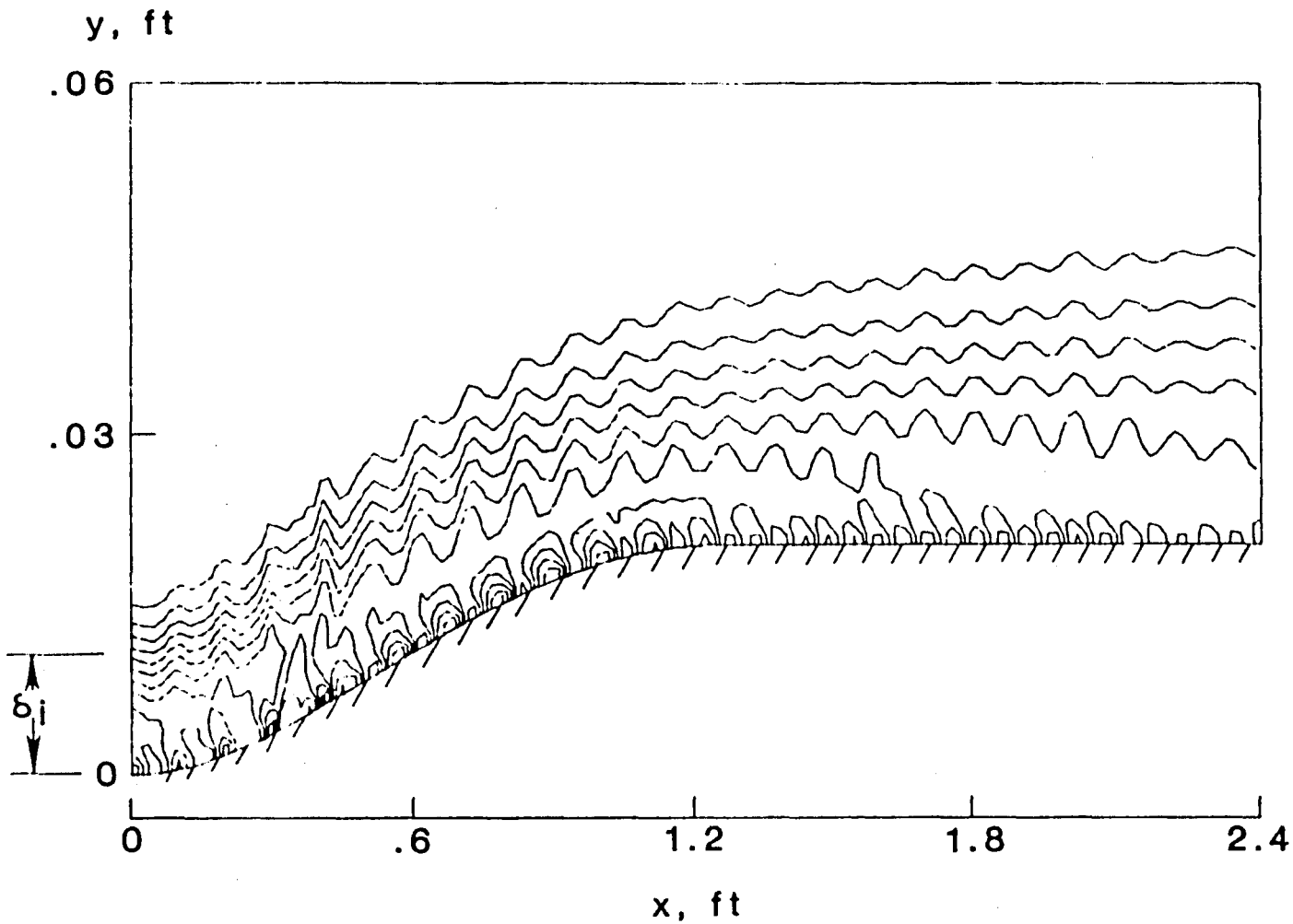


Figure 8. Instantaneous Total Vorticity Contours With Out-Of-Phase Heating, Configuration 1.

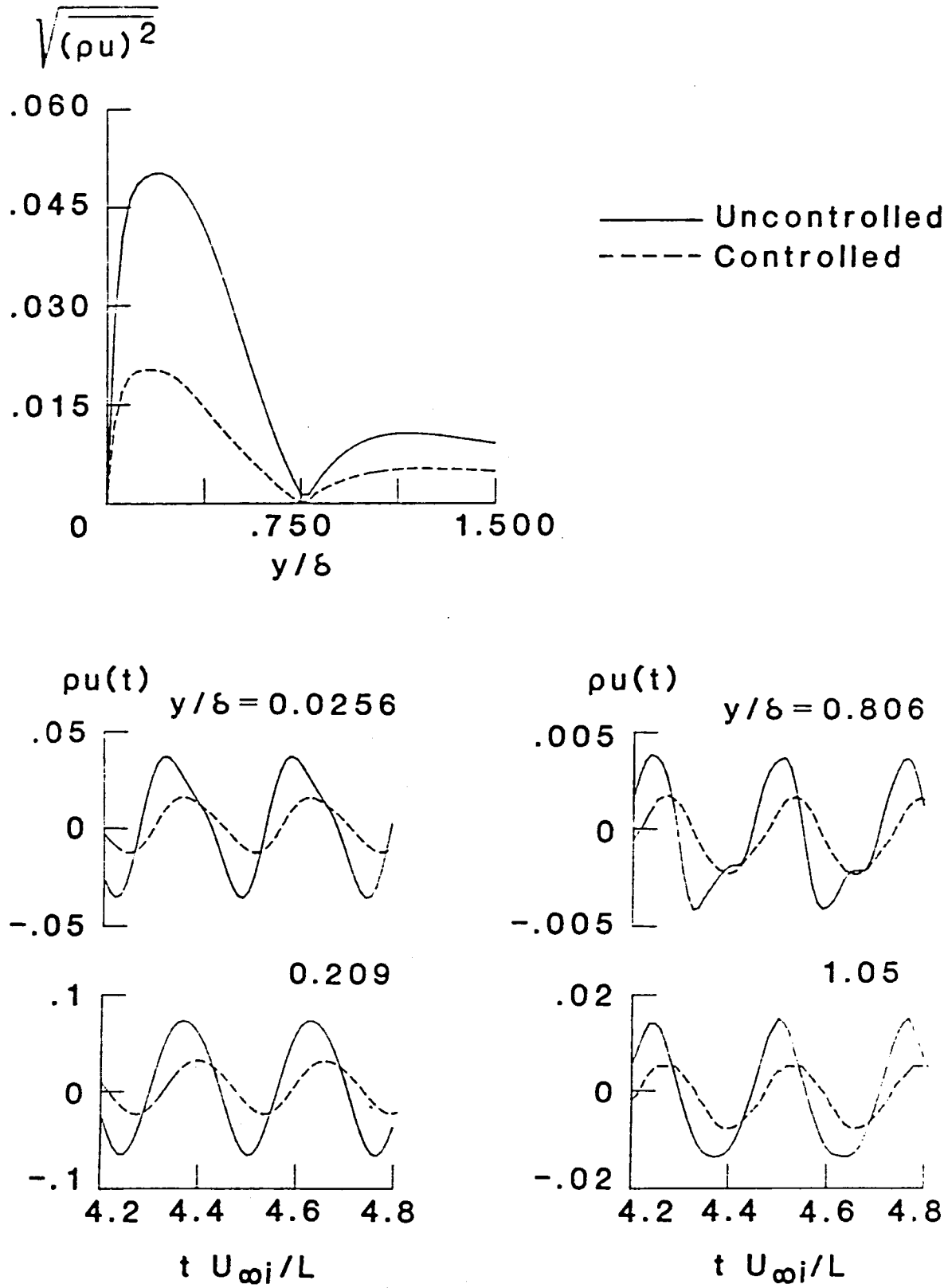


Figure 9. Effect of Control by Heating on RMS and instantaneous amplitude, x = 1.4 ft.

Standard Bibliographic Page

| 1. Report No. NASA CR-178143<br>ICASE Report No. 86-48 | 2. Government Accession No. | 3. Recipient's Catalog No. |
|---|---|---|
| 4. Title and Subtitle<br>STABILITY AND CONTROL OF COMPRESSIBLE FLOWS OVER A SURFACE WITH CONCAVE-CONVEX CURVATURE | | 5. Report Date<br>July 1986<br>6. Performing Organization Code |
| 7. Author(s)<br>Lucio Maestrello, Alvin Bayliss, Paresh Parikh, Eli Turkel | | 8. Performing Organization Report No.<br>86-48 |
| 9. Performing Organization Name and Address<br>Institute for Computer Applications in Science and Engineering<br>Mail Stop 132C, NASA Langley Research Center<br>Hampton, VA 23665-5225 | | 10. Work Unit No.<br>11. Contract or Grant No.<br>NAS1-17070, NAS1-18107 |
| 12. Sponsoring Agency Name and Address<br>National Aeronautics and Space Administration<br>Washington, D.C. 20546 | | 13. Type of Report and Period Covered<br>Contractor Report<br>14. Sponsoring Agency Code<br>505-31-83-01 |

15. Supplementary Notes

Langley Technical Monitor: J. C. South

Submitted to J. Fluid Mechanics

Final Report

16. Abstract

The active control of spatially unstable disturbances in a laminar, two-dimensional, compressible boundary layer over a curved surface is numerically simulated. The control is effected by localized time-periodic surface heating. We consider two similar surfaces of different heights with concave-convex curvature. In one, the height is sufficiently large so that the favorable pressure gradient is sufficient to stabilize a particular disturbance. In the other case the pressure gradient induced by the curvature is destabilizing. It is shown that by using active control that the disturbance can be stabilized. The results demonstrate that the curvature induced mean pressure gradient significantly enhances the receptivity of the flow to localized time-periodic surface heating and that this is a potentially viable mechanism in air.

| 17. Key Words (Suggested by Authors(s)) | 18. Distribution Statement |
|---|---|
| laminar flow, control, numerical method | 02 - Aerodynamics<br>34 - Fluid Mechanics and Heat Transfer<br><br>Unclassified - unlimited |

| 19. Security Classif.(of this report) | 20. Security Classif.(of this page) | 21. No. of Pages | 22. Price |
|---|---|---|---|
| Unclassified | Unclassified | 34 | A03 |

For sale by the National Technical Information Service, Springfield, Virginia 22161

NASA-Langley, 1986

**End of Document**